ELSEVIER

Journal of Quantitative Spectroscopy & Radiative Transfer 109 (2008) 269–279

Journal of Quantitative Spectroscopy & Radiative Transfer

www.elsevier.com/locate/jqsrt

# Monte Carlo simulation of radiative heat transfer and turbulence interactions in methane/air jet flames

Anquan Wang, Michael F. Modest*, Daniel C. Haworth, Liangyu Wang

*Department of Mechanical Engineering, Pennsylvania State University, University Park, PA 16802, USA*

Received 15 February 2007; accepted 31 August 2007

**Abstract**

A Photon Monte Carlo method combined with a composition PDF method is employed to model radiative heat transfer in combustion applications. Turbulence–radiation interactions (TRIs) can be fully taken into account using the proposed method. Sandia's Flame D and artificial flames derived from it are simulated and good agreement with experimental data is found. The effects of different TRI components are investigated. It is shown that, to predict the radiation field accurately, emission TRI must be taken into account, while, as expected, absorption TRI is negligible in the considered nonsooting methane/air jet flames if the total radiation quantities are concerned, but non-negligible for evaluation of local quantities. The influence of radiation on the turbulent flow field is also discussed.


*Keywords:* Thermal radiation; Monte Carlo methods; Turbulence–radiation interactions; Molecular gas; Flame

## 1. Introduction

Radiation tends to dominate the heat transfer process in many high-temperature applications, such as turbulent flames. In such cases radiation and turbulence are coupled processes. Turbulent fluctuations of temperature and species concentrations tend to enhance emission and heat loss, which have influence on temperature and density fields. The density field may further affect the turbulent flow field. The treatment of turbulence–radiation interactions (TRIs) is a challenging task because of the nonlinear coupling between temperature, species concentrations and radiative intensities. In traditional combustion simulations radiation and turbulence are treated as decoupled processes, using mean temperature and species concentration fields. However, many experimental and numerical results have shown that such treatment may result in underestimation of heat loss by a factor of up to three [1,2]. Therefore, TRIs must be taken into account in most combustion calculations.

TRIs include the nonlinear coupling between local blackbody intensity and local absorption coefficient and the nonlinear coupling of incident radiation and local absorption coefficient. The former coupling may be referred to as "emission TRI" and determined from local properties only, while the latter is referred to as

*Corresponding author. Fax: +1 814 863 4848.
*E-mail address:* mfm@engr.psu.edu (M.F. Modest).

0022-4073/$ - see front matter 
doi:10.1016/j.jqsrt.2007.08.030

"absorption TRI" and is governed by property fluctuations across the entire domain. Virtually all studies on TRIs to date have employed a major simplifying assumption, the so-called "optically thin fluctuation assumption" (OTFA) [3], which assumes that, if the eddies are optically thin and statistically independent, the local fluctuations in the absorption coefficient are uncorrelated from the fluctuations of radiation intensity passing through that eddy. By applying the OTFA, absorption TRI can be neglected and only two terms, the emission term (correlation of blackbody intensity and absorption coefficient) and the mean absorption coefficient, need to be closed.

Several approaches to close the above terms have been developed over the years. In his investigation of buoyant propane flames, Snegirev [4] ignored the fluctuations of species concentrations and expanded the gray absorption coefficient and emission term into Taylor series around mean temperatures, followed by truncation of high-order fluctuations. The truncation error was estimated by a model involving two model constants. Another more rigorous approach of emission TRI modeling was first proposed by Song and Viskanta in their investigation of a coupled reacting flow with radiation for a turbulent flame inside a two-dimensional natural gas furnace [5]. They evaluated the mean absorption coefficient and the emission term by employing a presumed Gaussian-shaped probability density function (PDF) of mixture fraction. Coelho et al. [6] followed Song and Viskanta's approach in the investigation of TRIs in a nonluminous turbulent jet diffusion flame, except that the PDF of mixture fraction was obtained from the solution of a flamelet model. The most promising approach appears to be the joint-probability-density-function (joint-PDF) method, which was first developed by Pope [7] to treat chemical sources in turbulent reacting flows. In this method any term can be evaluated exactly as long as it is a function of local scalars only (such as temperature, species concentrations, etc.), by solving the joint PDF of scalars using a particle Monte Carlo method [7,8], in which the flow is represented by a sufficiently large number of discrete particles (point-masses) evolving with time. Mazumder and Modest [9] used the joint velocity-composition PDF method to treat the emission TRI exactly in a bluff-body burner flame, since the emission term and absorption coefficient are functions of local scalars only. Although the velocity-composition PDF method is very powerful, it is still in its early stage of development. Therefore, Li and Modest [10] employed the more mature joint composition PDF method to treat the emission TRI exactly in turbulent jet flames. They used a commercial finite-volume (FV) CFD code to supply the mean flow field required by the particle Monte Carlo solution of the PDF transport equation.

To take absorption TRI fully into account, detailed knowledge of instantaneous fields of temperature and species concentrations is required. To date the only attempt to take the effects of absorption TRI into account was made by Tessé et al. [11] in their modeling of radiative transfer in a turbulent, sooty ethylene/air jet flame. First, they used a particle Monte Carlo method to obtain the three-dimensional PDF of the reaction progress variable, mixture fraction and soot volume fraction, by tracking fluid packets through the mean flow field. After that they assumed that the thermophysical properties of individual coherent turbulent structures were uniform and randomly obtained from the three-dimensional PDF to construct a joint composition PDF of temperature and concentrations for each individual turbulent structure. Finally, a Monte Carlo ray tracing scheme was carried out, in which ray paths were divided by turbulent structures into continuous segments, in which the radiative properties were evaluated from the corresponding joint PDF, and absorption TRI was taken into account without invoking the OTFA. However, the composition PDF was obtained in a fairly complicated way, which tends to be CPU and memory inefficient, rather than by solving the composition PDF transport equation using the particle Monte Carlo method directly. In addition, smaller scales of turbulence were neglected since they assumed that the turbulent structures of the flame were homogeneous to simplify ray tracing.

In the present paper a new approach is proposed to take both emission and absorption TRI fully into account. Similar to Li and Modest [10], we employ a hybrid FV/PDF method, in which the composition PDF transport equation is solved by the particle Monte Carlo method [7,8]. The instantaneous particle field in the PDF method is assumed to be a snapshot of the real turbulent flow field and, therefore, the scalars carried by particles represent instantaneous turbulent fields of temperature and concentrations. As a result, both the emission and the absorption TRIs can be taken into account by using a photon Monte Carlo (PMC) method for the radiative transfer without making any further assumptions. The PMC method employed in the present work was developed recently by Wang and Modest [12,13] for media represented by particle fields.

## 2. Composition PDF method

In composition PDF methods physical scalars, including temperature and species concentrations, are treated as independent random variables. The joint PDF is then a function of spatial location, time and composition space. Once the joint PDF is obtained at a certain position $\underline{x}$ and time instant $t$, the mean value for any function, $Q$, of these scalars can be evaluated exactly as

$$\langle Q(\underline{\phi})\rangle = \int_{-\infty}^{\infty} Q(\underline{\psi}) f(\underline{\psi};\underline{x},t)\,\mathrm{d}\,\underline{\psi}\,, \tag{1}$$

where $\underline{\phi}$ is the vector of physical scalars, $\underline{\psi}$ is the corresponding random variable vector, $Q$ is a function of $\underline{\phi}$ only and $f$ is the joint PDF, which represents the probability density of a compound event $\underline{\phi}=\underline{\psi}$. In practice the mass density PDF, $\mathscr{F}(\underline{\psi};\underline{x},t)=\rho(\underline{\psi};\underline{x},t)f(\underline{\psi};\underline{x},t)$, is more convenient and frequently used and its transport equation can be derived based on the conservation of scalars as [10]

$$\begin{aligned}&\frac{\partial\mathscr{F}}{\partial t}+\frac{\partial}{\partial x_i}[\tilde{u}_i\mathscr{F}]+\frac{\partial}{\partial\psi_\alpha}[S_{\alpha,\mathrm{rea}}(\underline{\psi})\mathscr{F}]\\&\quad=-\frac{\partial}{\partial x_i}[\langle u_i''\,|\,\underline{\psi}\rangle\mathscr{F}]+\frac{\partial}{\partial\psi_\alpha}\left[\left\langle\frac{1}{\rho}\frac{\partial J_i^\alpha}{\partial x_i}\middle|\,\underline{\psi}\right\rangle\mathscr{F}\right]-\frac{\partial}{\partial\psi_s}[\langle S_{\mathrm{rad}}\,|\,\underline{\psi}\rangle\mathscr{F}],\end{aligned} \tag{2}$$

where $i$ and $\alpha$ are summation indices in physical space and composition space, respectively, and $\langle A|B\rangle$ is the conditional mean of the event $A$, given that the event $B$ occurs. Variables with tildes and double primes are Favre means of the variables and fluctuations about them. Terms appearing on the left-hand side of (2) can be accounted for exactly. The first two terms are the rate of change and the advection of the PDF in the Favre-averaged mean flow. The third term is the transport of PDF in composition space due to chemical reactions. Terms on the right-hand side must be modeled. The first two terms represent the transport in physical space due to turbulent convection and transport in composition space due to molecular mixing, respectively, and are commonly modeled using the gradient-diffusion hypothesis and a pair-exchange mixing model [7,14] as

$$\begin{aligned}&\langle u_i''|\psi\rangle\mathscr{F}\simeq-\Gamma_{\mathrm{T}}\frac{\partial\mathscr{F}}{\partial x_i},\\&\frac{\partial}{\partial\psi_\alpha}\left[\left\langle\frac{1}{\rho}\frac{\partial J_i^\alpha}{\partial x_i}\middle|\,\underline{\psi}\right\rangle\mathscr{F}\right]\simeq 2C_\phi\omega\left[2\int_0^\infty\mathscr{F}(\underline{\psi}+\underline{\psi}')\mathscr{F}(\underline{\psi}-\underline{\psi}')\,\mathrm{d}\underline{\psi}'-\mathscr{F}(\underline{\psi})\right],\end{aligned} \tag{3}$$

where $\Gamma_{\mathrm{T}}=c_\mu\langle\rho\rangle\sigma_\phi k^2/\varepsilon$ is the turbulent diffusivity, $k$ and $\varepsilon$ are the turbulent kinetic energy and its dissipation rate, $c_\mu$ and $\sigma_\phi$ are a model constant in the $k$–$\varepsilon$ turbulence model and turbulent Schmidt or Prandtl number, respectively; $\omega=\varepsilon/k$ is a turbulent "frequency" and $C_\phi$ is a constant in the mixing model.

The third term on the right-hand side of Eq. (2) is the transport of the composition PDF due to radiative transfer. The radiative source is the difference between the energy gain due to absorption of incident radiation and energy loss due to local emission as

$$S_{\mathrm{rad}}=\int_0^\infty\kappa_\eta(G_\eta-4\pi I_{b\eta})\,\mathrm{d}\eta,\quad G_\eta=\int_{4\pi}I_\eta\,\mathrm{d}\Omega, \tag{4}$$

where $\kappa_\eta$ is the local spectral absorption coefficient, $I_{b\eta}$ is the local spectral blackbody intensity and $G_\eta$ is the incident radiative intensity integrated over the entire solid angle of $4\pi$. Both $\kappa_\eta$ and $I_{b\eta}$ are functions of local composition variables only and, therefore, can be evaluated exactly. In contrast, $G_\eta$ depends on the properties at every point in the domain, and the one-point PDF employed here is not sufficient to close this term. However, as mentioned earlier, the PDF transport equation (2) is usually solved by particle Monte Carlo methods, in which the PDF is discretized into a sufficiently large number of delta functions (particles) carrying their own scalars. These particles are traced and scalars carried are mixed over time according to the Lagrangian form of Eq. (2) [7]. If we assume that the instantaneous particle field represents a snapshot of real flow, a PMC method can be employed to evaluate both the local emission ($4\pi\kappa_\eta I_{b\eta}$) and the absorption of incident radiation ($\kappa_\eta G_\eta$) without any further simplification. It is worth noting that emission is fundamentally closed using the one-point PDF and does not require modeling. However, emission is automatically treated in the PMC method.

## 3. PMC methods

### 3.1. Radiative transfer modeling

PMC methods directly simulate the physical processes, i.e., emission, absorption, scattering and reflection, by releasing representative photons bundles (rays) into random directions, which are traced until they are absorbed at certain points in the medium or escape from the domain. Traditional PMC methods developed for continuous media are not useful for radiation simulations in PDF methods, since the media are represented by discrete particle fields (point-masses). To alleviate this problem, PMC schemes for media represented by particle fields were recently developed by Wang and Modest [12,13]. In their series of works they developed several emission and absorption schemes as well as techniques of statistical error reduction for PMC simulations in particle fields.

Since the medium is represented by particles, rays are released in random directions from particles to model particle emission. The total emitted energy of particle $i$ is calculated from

$$Q_{\mathrm{emi},i} = 4\kappa_{\rho,i} m_i \sigma T_i^4, \tag{5}$$

where $\kappa_{\rho,i}$ is the density-based Planck-mean absorption coefficient at particle temperature $T_i$, $\sigma$ is the Stefan–Boltzmann constant and $m_i$ is the mass. If self-absorption is considered, a more sophisticated expression of the total emission can be obtained from Chapter 9.9 of Modest [15]. Obviously, particles have different total emission, varying over several orders of magnitude, due to the inhomogeneity in the flame. If particles emit the same number of rays, each ray would represent considerably different amounts of energy and the simulation would become inefficient with large statistical errors. In order to reduce such errors, Wang and Modest [13] developed an adaptive emission scheme to limit the ray energy to a small range, in which particles with high emission release more rays while particles with very low emission are combined to emit a single ray. Using this emission scheme statistical errors were reduced by factors of five to six in a frozen field study of a methane/air flame mentioned earlier.

One of the difficulties of ray tracing in particle fields is the evaluation of optical thickness, that the ray travels through, which requires interactions between the ray and particles. In Wang and Modest's work [12] influence regions are assigned to either the ray or the particle or both, in order to simulate the ray–particle interaction. If the ray is not assigned an influence region, its energy propagates one-dimensionally along a line, which is the standard ray model in traditional PMC methods. Otherwise, a small conical solid angle is assigned to the ray, and the ray energy propagates axisymmetrically along the cone, with its strength decaying in the radial direction normal to the cone axis, for which a normalized two-dimensional center-symmetric weight function is utilized. Influence regions can also be assigned to particles. Normalized three-dimensional spherical weight functions are often used to model particle influence regions, which is referred to as "spherical particle model (SPM)". A special case of this particle model assumes the particle density to be constant in its influence region, which is referred to as "constant-density spheres (CDS)" model. Another particle model is the so-called "point particle model (PPM)," in which no influence region is assigned to particles and particles remain as point-masses. The advantage of this model is that no other assumption is employed for particles and, therefore, it will not induce any inconsistency with the PDF method. The disadvantage of this model is that it is difficult to determine the interaction of a photon ray with a point-mass. Based on the above ray and particle models, Wang and Modest [12] proposed three ray–particle interaction schemes to model the absorption, namely the cone-PPM, cone-CDS and line-CDS models. The three absorption models were shown to be equivalent in terms of statistical errors. The cone-PPM model will be adopted in the present study, since it does not introduce any inconsistency with the PDF method. Based on this model, the optical thickness that a ray $j$ travels through during its interaction with a particle $i$ is evaluated as

$$\Delta\tau_{ij} = \frac{\kappa_{\rho,i} W_{ij} m_i}{\pi R_{\mathrm{c},ij}^2}, \tag{6}$$

where $\kappa_{\rho,i}$ is the density-based absorption coefficient of particle $i$, $m_i$ is the mass of particle $i$, $R_{\mathrm{c},ij}$ is the local cross-sectional radius of ray $j$ at the location of particle $i$ and $W_{ij}$ is the weight of particle $i$ in ray $j$ and is computed from the normalized two-dimensional center-symmetric weight function, which models the decaying

strength of ray energy in the radial direction. The total optical thickness that ray $j$ travels through is accumulated as

$$\tau_j = \sum_{i \in I_j} \Delta\tau_{ij}, \tag{7}$$

where $I_j$ denotes all particles that ray $j$ interacts with along its path. Wang and Modest [12,13] proposed two Monte Carlo approaches to distribute the ray energy among the particles it interacts with. In the standard Monte Carlo method a random number is drawn to determine the optical thickness ray $j$ can travel through before it is absorbed. As ray $j$ travels through the medium, as soon as the total optical thickness evaluated from Eq. (7) exceeds its predetermined value, all the energy the ray carries is dumped into the last particle it interacts with. If this does not occur before ray $j$ leaves the domain, its energy contributes to the heat loss from the domain. This method is inefficient for optically thin flames, such as the methane/air flames under investigation, so that most photon bundles would exit the domain without any contribution to the statistics inside the medium. This can be alleviated by the so-called "energy-partitioning" method [16], in which the energy carried by a ray is not absorbed by a single particle, but rather is attenuated gradually along its path, by distributing its energy to all the particles it interacts with, until its depletion or until it leaves the domain. If a ray leaves the domain, its remaining energy contributes to the heat loss from the domain. Wang and Modest [13] compared these two methods in a frozen field study of a methane/air flame and demonstrated that the energy-partitioning method can decrease the statistical errors by a factor of two to three at a cost of slightly increased CPU time, using the same total number of rays. By employing the energy-partitioning method, the total energy absorbed by particle $i$ is calculated as

$$Q_{\mathrm{abs},i} = \sum_{j \in J_i} Q_j^{(i)} [1 - \exp(-\Delta\tau_{ij})], \tag{8}$$

where $J_i$ denotes all the rays that interacted with particle $i$ and $Q_j^{(i)}$ is the energy carried by ray $j$ just before interacting with particle $i$.

Required by the overall energy equation in the combustion model, the cell-mean radiative heat source term needs to be evaluated from the underlying particle field. According to an energy balance for an FV cell, the amounts of radiative energy entering and leaving the cell must be balanced by the energy emitted and absorbed by particles in the cell. Thus, the cell-mean radiative heat source term can be derived as

$$\langle S_{\mathrm{rad}} \rangle = \frac{1}{V_c} \sum_{i \in I_c} (Q_{\mathrm{abs},i} - Q_{\mathrm{emi},i}), \tag{9}$$

where $V_c$ is the cell volume and $I_c$ denotes the particles in the cell.

### 3.2. Spectral modeling

Wang and Modest [17] also developed a line-by-line (LBL) spectral model for Monte Carlo simulations. The LBL method is an exact method for spectral modeling, but the direct spectral integration usually is too time consuming when combined with traditional RTE solution methods and thus not practical for radiation calculations, since there are millions of spectral lines across the spectrum. Over the years, many spectral models have been developed to approximate the spectral variation of absorption coefficients at much smaller computational cost, among which the full-spectrum $k$-distribution (FSK) method [18] is the most advanced. In the FSK method the oscillating absorption coefficient is reordered into a monotonic $k$-distribution, which can be efficiently integrated using few quadrature points. While this method is exact for homogeneous media, it results in errors for inhomogeneous media, such as in flames, since it is based on the correlatedness of absorption coefficients and this correlatedness breaks down in the presence of large gradients of temperature and species concentrations. It has been shown by Wang and Modest [17] that the FSK method may result in more than 10% error in emission and absorption calculations in some extreme cases and about 3% in a methane/air flame. In the LBL MC scheme employed in the present study, rather than performing direct spectral integration, the wavenumber carried by the ray is determined randomly before it is traced. By random wavenumber determination, wavenumbers that contribute most to the emission are more frequently chosen.

Therefore, this method does its own reordering similar to the FSK method, and the number of spectral locations required is greatly reduced.

In the LBL MC scheme the wavenumber determination is done by the inversion of a random-number relation $R_\eta - \eta$. Instead of calculating the mixture random-number relation directly, it is assembled from species random-number relations. The species random numbers are calculated as

$$R_{\eta,s} = \frac{\pi}{\kappa_{p,s}\sigma T^4}\int_0^\eta \kappa_{p\eta,s} I_{b\eta}\,\mathrm{d}\eta, \tag{10}$$

where $R_{\eta,s}$ is a random number uniformly distributed in $[0,1)$, $\kappa_{p\eta,s} = \kappa_{\eta,s}/p_s$ is the pressure-based spectral absorption coefficient and $p_s$ is the partial pressure of species $s$, $\kappa_{p,s}$ is the pressure-based Planck-mean absorption coefficient and $T$ is the gas temperature. The species random-number relations and species absorption coefficients can be tabulated beforehand, so that mixture values can be efficiently calculated to determine emission wavenumbers and absorption coefficients during ray tracing, from

$$R_\eta = \sum_s x_s\kappa_{p,s}R_{\eta,s}\Big/\sum_s x_s\kappa_{p,s}, \quad \kappa_{p\eta} = \sum_s x_s\kappa_{p\eta,s}, \tag{11}$$

where $x_s$ is the mole fraction of species $s$. In the present study, species random-number relation $R_{\eta,s}$ and the pressure-based absorption coefficient $\kappa_{p\eta,s}$ are tabulated at a spectral resolution not less than $0.01\,\mathrm{cm}^{-1}$ for two species (water vapor and carbon dioxide), 23 temperatures (ranging from 300 to 2500 K) and a few mole fractions (2 for water vapor and 1 for carbon dioxide).

## 4. Flame simulations

Sandia's Flame D [19] and derived flames similar to the ones discussed in Li and Modest [20] have been investigated here using the proposed method. The experimental setup of the Flame D is summarized as follows: the fuel jet (diameter $d_j = 7.2\,\mathrm{mm}$) with high velocity ($u_j = 49.6\,\mathrm{m/s}$) is surrounded by an annular pilot flow ($d_\mathrm{p} = 18.4\,\mathrm{mm}$, $u_\mathrm{p} = 11.4\,\mathrm{m/s}$), and a slow outer coflow of air ($u_\mathrm{c} = 0.9\,\mathrm{m/s}$); the fuel is a mixture of air and methane with a volume ratio of 3:1. The other two considered (artificial) flames were derived from Flame D by doubling and quadrupling the jet diameter to increase the flame optical thickness while keeping the Reynolds number constant (i.e., decreasing velocities). For future reference we denote the Flame D as $\kappa L.1$, the doubled flame as $\kappa L.2$ and the quadrupled flame as $\kappa L.3$, following the naming system by Li and Modest [20]. In comparison to Li and Modest's work, we used a more advanced composition PDF code with mass-consistency and enthalpy-consistency algorithms built in [21] and a more realistic chemical reaction mechanism involving 16 species and 41 steps [22] versus their single-step mechanism. In Li and Modest's simulations the Damköhler number of $\kappa L.2$ and $\kappa L.3$ was kept identical to that of $\kappa L.1$ by artificially decreasing the reaction rates. Here, we used the same multi-step chemical mechanism for all three flames (with corresponding increase in Damköhler number). For radiation, Li and Modest used the P-1 method to solve the RTE and the FSK method for spectral modeling, which are less accurate than the models employed here.

In the present study, a wedge-like three-dimensional grid system consisting of 2730 hexahedron cells is employed to simulate the two-dimensional axisymmetric flames by applying periodic boundary conditions on the sides, as shown in Fig. 1. The azimuthal angle is 10° and its dimensions in $x$- and $z$-directions are $20d_j$ and $100d_j$, respectively. The grid is designed to be very fine in the fuel jet at the inlet to resolve the large local gradients, and coarser in the air coflow and downstream to save computational time. In the particle Monte Carlo method, different cells are controlled to contain roughly the same number of particles to have similar

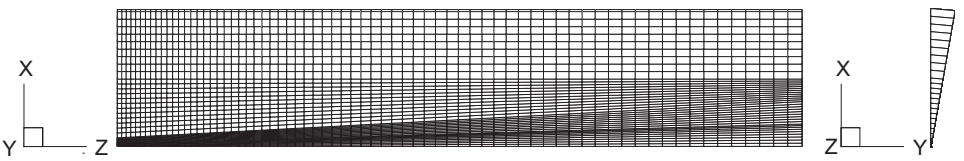


Fig. 1. Grid system used in flame simulations.

statistical variations. It was found that around 30 particles per cell on average are sufficient to resolve turbulence fluctuations in the considered flames. Therefore, roughly 80,000 particles are used to populate the entire computational domain. For the radiation simulation the cone-PPM absorption scheme is used in the PMC method. The cone opening angle needs to be chosen appropriately, since a too small opening angle may cause too few particles to interact with the ray, resulting in a large statistical error, while a large opening angle may smooth out turbulence. A $1^\circ$ opening angle is used here, as recommended by Wang and Modest [12]. The inlet and the side boundary are treated as cold and black since the air is at the ambient temperature, while the exit is assumed to be diffusely reflective, since the hot gas downstream outside of the domain may emit energy back into the domain. At any given time step only about 80,000 photon bundles are traced. Therefore, to feed back the cell means of the radiative source to the enthalpy equation in the FV code, the time-averaged cell means are fed back to reduce CPU time, since the flames are statistically stationary. It was found that tracing more photon bundles per time step would considerably increase the CPU requirements while simulation results remain almost unchanged. In traditional FV methods the residual error diminishes to zero with sufficient number of iterations, and can be used as a criterion of convergence. However, the residual error in hybrid FV/Monte Carlo method unlikely diminishes to zero due to the statistical scatter. Therefore, it is impossible to use the residual error as a criterion of convergence. The emission-averaged temperature and the volume-averaged root-mean-square (rms) temperature fluctuation are used here to monitor the convergence, i.e.,

$$\langle T\rangle_{\mathrm{e}} = \int_V \kappa_{\mathrm{p}} T^5 \mathrm{d}V \Big/ \int_V \kappa_{\mathrm{p}} T^4 \mathrm{d}V \quad \text{and} \quad \langle T''\rangle_{\mathrm{v}} = \frac{1}{V}\sum_c \left[\frac{V_c}{\rho_c}\sum_{p\in c} m_{\mathrm{p}}(T_{\mathrm{p}} - T_c)^2\right]^{1/2}, \tag{12}$$

where $m_{\mathrm{p}}$ and $T_{\mathrm{p}}$ are the particle mass and temperature, respectively, $\rho_c$ and $T_c$ are cell-mean density and temperature, respectively, and $V$ is the total volume of the domain. Fig. 2 shows the variations of the so-defined average temperature and temperature fluctuation during the simulation of the $\kappa L.1$ flame with a time step of 50 μs. The temperature fluctuation converges much slower than the temperature since it is a higher order moment.

The importance of radiation in the considered flames is demonstrated in Fig. 3. The centerline mean temperature profiles evaluated with and without radiation are presented for all three flames. It is shown that

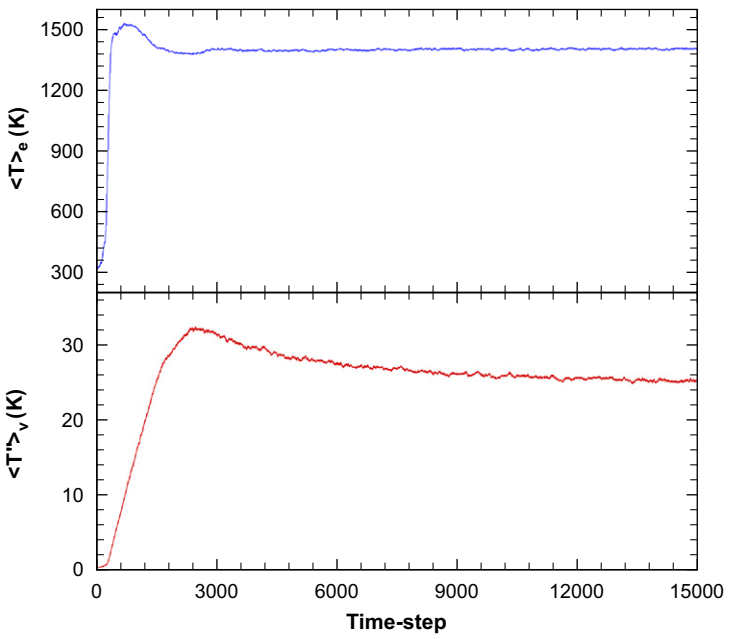


Fig. 2. Convergence check in simulation of $\kappa L.1$ flame.

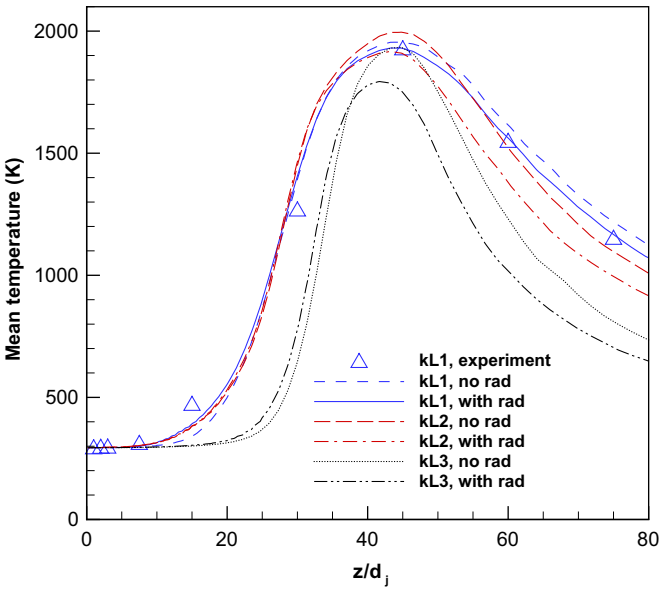


Fig. 3. Centerline profiles of mean temperature in considered flames.

Table 1
Emission-averaged flame temperatures using different radiation treatments (in K)

| Flames | No radiation | No-TRI | Partial-TRI | Full-TRI |
|---|---|---|---|---|
| $\kappa L.1$ | 1407 | 1402 | 1395 | 1394 |
| $\kappa L.2$ | 1466 | 1424 | 1420 | 1418 |
| $\kappa L.3$ | 1484 | 1415 | 1403 | 1396 |

radiation has a cooling effect, making the flames shorter. The importance of radiation, implied by the difference between profiles with and without radiation, becomes more and more significant as the flame optical thickness increases from $\kappa L.1$ to $\kappa L.3$. In the simulation of the $\kappa L.1$ flame, to match the experimental data better, the value of $C_{\varepsilon 1}$, a constant in the $k$–$\varepsilon$ model, is chosen to be 1.48 rather than the standard value of 1.44. The same value is then employed in both $\kappa L.2$ and $\kappa L.3$ flames. Our result matches the experimental data much better than those of Li and Modest [20], due to a more advanced composition PDF method, the more detailed chemical mechanism and more accurate radiation models. Since all three of Li and Modest's flames have identical Reynolds and Damköhler numbers, they are statistically identical if radiation is ignored. In our $\kappa L.2$ and $\kappa L.3$ simulations with realistic chemistry the Damköhler number increases by a factor of four and 16, respectively.

The effects of TRIs have also been investigated. If the particle properties (temperature and absorption coefficient) are employed in both the emission and the absorption calculations, both emission TRI and absorption TRI can be taken into account, called "full-TRI". If the particle properties are used in the emission calculations and the cell-mean values are used in the absorption calculations, only emission TRI is taken into account, which is equivalent to the OTFA assumption and is called here "partial-TRI". If cell-mean values are used in both the emission and the absorption calculations, TRIs are neglected completely, and we call it "no-TRI". Table 1 collects the emission-averaged flame temperatures with different TRI treatments as well as without radiation. Once again, the effect of radiation on flame temperature becomes more significant as the flame optical thickness increases. The effect of absorption TRI, reflected by the difference between full-TRI and partial-TRI treatments, also becomes more and more non-negligible as the flame optical thickness increases. However, the effects of different TRI treatments on the averaged temperature are not prominent, since all three flames are optically thin. Table 2 shows the total emission and net radiative heat loss using

Table 2
Total emission and net radiative heat loss using different TRI treatments (in kW)

| Flames | No-TRI | | Partial TRI | | | Full-TRI | | |
|---|---|---|---|---|---|---|---|---|
| | $\dot{Q}_{em}$ | $\dot{Q}_{net}$ | $\dot{Q}_{em}$ | $\dot{Q}_{net}$ | Δ TRI (%) | $\dot{Q}_{em}$ | $\dot{Q}_{net}$ | Δ TRI (%) |
| $\kappa L.1$ | 0.849 | 0.500 | 1.07 | 0.648 | 29.6 | 1.07 | 0.645 | 29.0 |
| $\kappa L.2$ | 5.01 | 2.57 | 6.22 | 3.29 | 28.0 | 6.24 | 3.27 | 27.2 |
| $\kappa L.3$ | 17.44 | 8.48 | 22.94 | 11.57 | 36.4 | 22.95 | 11.37 | 34.1 |

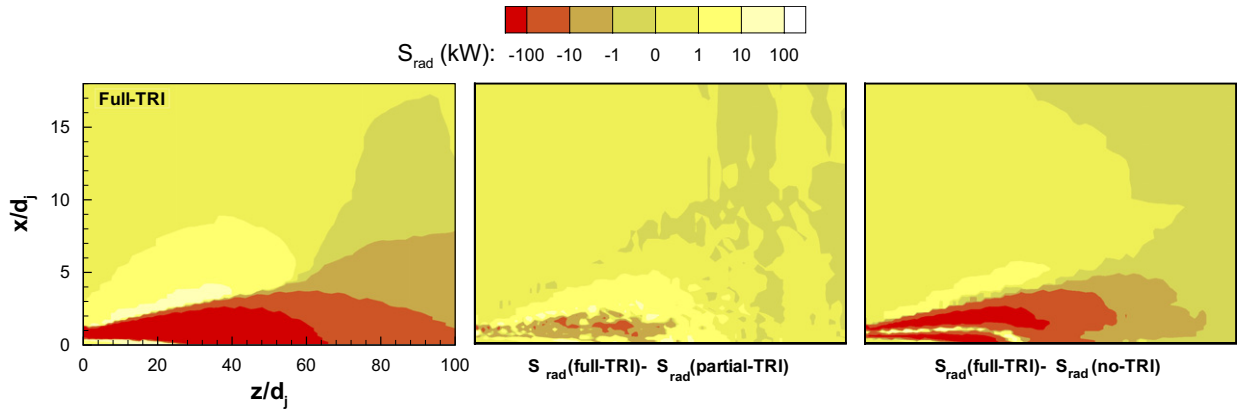


Fig. 4. Radiative heat source in $\kappa L.3$ flame.

different TRI treatments. The TRI effects, ΔTRI, are measured using the relative difference of net radiative loss between TRI treatments and the treatment without TRI. It is observed that the radiative heat loss increases by around 30% or more if emission TRI is taken into account, while absorption TRI (difference between full-TRI and partial-TRI treatments) is minor, which implies that all three flames are optically thin and the OTFA assumption is still valid, at least as far as total radiation (integrated over entire spectrum and domain) is concerned. The importance of different TRI components also can be demonstrated by comparing radiative heat sources (absorption minus emission) between different TRI treatments, as shown in Fig. 4. The contour plot in the left of Fig. 4 shows the cell-mean radiative sources with full-TRI for the $\kappa L.3$ flame. The heat source is strongly negative throughout the hot region of the flame, indicating a net radiative loss from the hot core, and positive outside the flame, indicating net absorption by the combustion products in this region. Further away the heat source is close to zero since there are no emitting–absorbing species there. The center frame shows the difference between full- and partial-TRI, i.e., the effects of absorption TRI. It is seen that absorption TRI is positive in the flame sheet region, indicating that increased emission due to emission TRI is countered by increased absorption due to absorption TRI. This phenomenon was also reported by Mehta and Modest [23] in their modeling of absorption TRI in optically thick eddies. They found that absorption TRI is very important in the active flame sheet region in optically thick spectral regions, although the total contribution to the overall radiative losses may be small. The contour plot on the right shows the effect of (emission plus absorption) TRI on the radiative heat source, indicating that TRI substantially increases heat loss from hot zones, while slightly increasing absorption outside the flame.

As mentioned earlier, radiation and turbulence are coupled processes. We have already shown that the turbulent fluctuations of temperature and species concentrations enhance radiative heat transfer. On the other hand, radiation tends to suppress temperature fluctuations and, consequently, density fluctuations, resulting in a reduced turbulence level in the flow field. Fig. 5 compares the axial rms temperature fluctuations and turbulence kinetic energy ($k$) for different radiation treatments. As shown in Fig. 5(a), the difference in temperature fluctuations between the full-TRI and no-radiation treatments is very small for the $\kappa L.1$ flame, since it is an optically very thin flame. For an optically thicker flame, such as $\kappa L.3$, radiation effects are a little

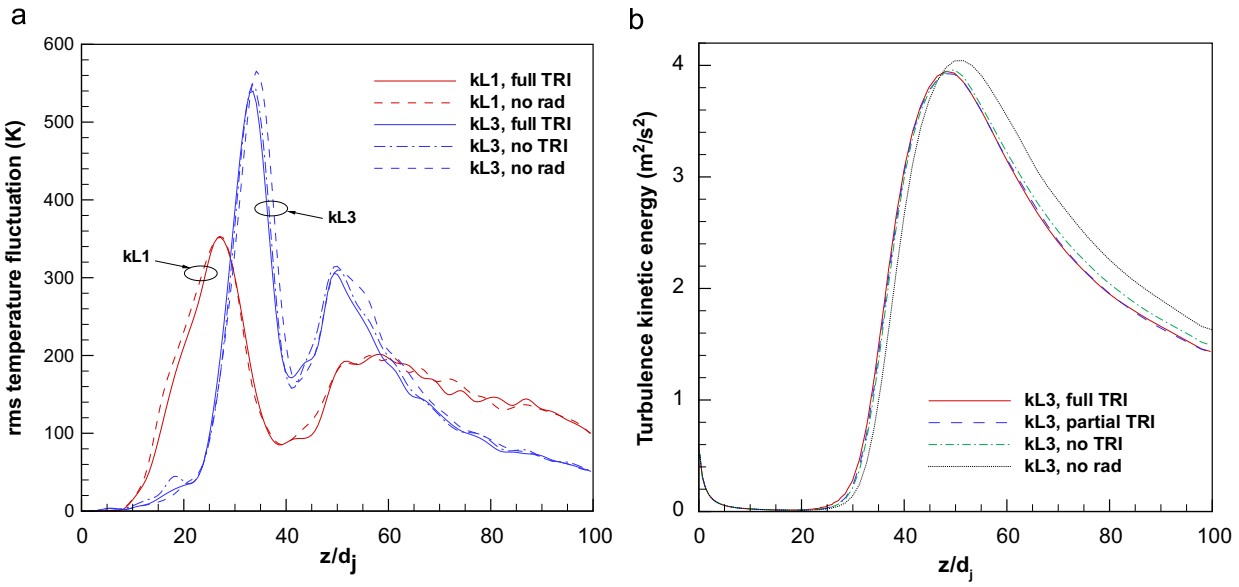


Fig. 5. Centerline profiles of root-mean-square (rms) temperature fluctuation and turbulence kinetic energy.

bit more prominent with reduced temperature fluctuations and flame length. The fact that rms temperature fluctuations are much larger for the $\kappa L.3$ flame is due to larger gradients of mean temperature in the $\kappa L.3$ flame. If TRI are also taken into account, temperature fluctuations are further suppressed by a small amount as shown in Fig. 5(a). As a result, the turbulence kinetic energy is reduced accordingly in the flow field as shown in Fig. 5(b). Once again, the effect of absorption TRI on turbulence kinetic energy is negligible.

## 5. Summary

The composition PDF method was employed to investigate radiative heat transfer in turbulent methane/air jet flames. A particle Monte Carlo method was utilized to solve the PDF transport equation. By assuming that the particle field represents instantaneous realizations of the flow field, a PMC method was employed to take both the emission and the absorption TRIs fully into account. Sandia's Flame D ($\kappa L.1$) and artificial flames ($\kappa L.2$ and $\kappa L.3$) derived from it were investigated using the new method. The centerline mean temperature profile obtained from the simulation matches the experimental data for Flame D very well. It was shown that radiation effects become more and more significant as the flame optical thickness increases from $\kappa L.1$ to $\kappa L.3$. Turbulence tends to enhance radiative heat transfer and radiative heat loss would be severely underpredicted if TRIs are neglected. By separating different TRI components in the considered flames, it was found that emission TRI must always be taken into account, while absorption TRI is relatively minor and the OTFA assumption is still valid for calculation of overall quantities, such as the net radiative heat loss, but has significant effects on local quantities in the flame. It was also observed that radiation and TRI tend to smooth out turbulence in the flow field.

## Acknowledgment

This research was sponsored by National Science Foundation under Grant number CTS-0121573.

## References

[1] Faeth GM, Gore JP, Chuech SG, Jeng SM. Radiation from turbulent diffusion flames. In: Annual review of numerical fluid mechanics and heat transfer, vol. 2. Washington, DC: Hemisphere; 1989. p. 1–38.

[2] Kounalakis ME, Gore JP, Faeth GM. Turbulence/radiation interactions in nonpremixed hydrogen/air flames. In: The 22nd symposium (international) on combustion, The Combustion Institute; 1988. p. 1281–90.
[3] Kabashnikov VP, Myasnikova GI. Thermal radiation in turbulent flows—temperature and concentration fluctuations. Heat Transfer—Sov Res 1985;17(6):116–25.
[4] Snegirev AY. Statistical modeling of thermal radiation transfer in buoyant turbulent diffusion flames. Combust Flame 2004;136:51–71.
[5] Song TH, Viskanta R. Interaction of radiation with turbulence: application to a combustion system. J Thermophys Heat Transfer 1987;1(1):56–62.
[6] Coelho PJ, Teerling OJ, Roekaerts D. Spectral radiative effects and turbulence/radiation interaction in a non-luminous turbulent jet diffusion flame. Combust Flame 2003;133:75–91.
[7] Pope SB. PDF methods for turbulent reactive flows. Prog Energy Combust Sci 1985;11:119–92.
[8] Subramaniam SV, Haworth DC. A PDF method for turbulent mixing and combustion on three-dimensional unstructured deforming meshes. Int J Engine Res 2000;1:171–90.
[9] Mazumder S, Modest MF. Turbulence–radiation interactions in nonreactive flow of combustion gases. ASME J Heat Transfer 1999;121:726–9.
[10] Li G, Modest MF. Application of composition PDF methods in the investigation of turbulence–radiation interactions. JQSRT 2002;73(2–5):461–72.
[11] Tessé L, Dupoirieux F, Taine J. Monte Carlo modeling of radiative transfer in a turbulent sooty flame. Int J Heat Mass Transfer 2004;47:555–72.
[12] Wang A, Modest MF. Photon Monte Carlo simulation for radiative transfer in gaseous media represented by discrete particle fields. ASME J Heat Transfer 2006;128(10):1041–9.
[13] Wang A, Modest MF. An adaptive emission model for Monte Carlo ray-tracing in participating media represented by statistical particle fields. JQSRT 2007;104(2):288–96.
[14] Curl RL. Dispersed phase mixing. 1. Theory and effects in simple reactors. AIChE J 1963;9(2):175–81.
[15] Modest MF. Radiative heat transfer. 2nd ed. New York: Academic Press; 2003.
[16] Modest MF. Determination of radiative exchange factors for three dimensional geometries with nonideal surface properties. Numer Heat Transfer 1978;1:403–16.
[17] Wang A, Modest MF. Spectral Monte Carlo models for nongray radiation analyses in inhomogeneous participating media. Int J Heat Mass Transfer 2007;50(19–20):3877–89.
[18] Modest MF. Narrow-band and full-spectrum $k$-distributions for radiative heat transfer—correlated-$k$ vs. scaling approximation. JQSRT 2003;76(1):69–83.
[19] Barlow RS, Frank JH. Effects of turbulence on species mass fractions in methane–air jet flames. In: Proceedings of the 27th symposium (international) on combustion. The Combustion Institute; 1998. p. 1087–95.
[20] Li G, Modest MF. Importance of turbulence–radiation interactions in turbulent diffusion jet flames. ASME J Heat Transfer 2003;125:831–8.
[21] Zhang YZ, Haworth DC. A general mass consistency algorithm for hybrid particle/finite-volume PDF methods. J Comput Phys 2004;194:156–93.
[22] Yang B, Pope SB. An investigation of the accuracy of manifold methods and splitting schemes in the computational implementation of combustion chemistry. Combust Flame 1998;112(1–2):16–32.
[23] Mehta R, Modest MF. Modeling absorption TRI in optically thick eddies. In: Proceedings of Eurotherm seminar 78, Poitiers, France, Amsterdam: Elsevier; April 2006.